DSA to grow electrochemically active biofilms of *Geobacter sulfurreducens*

Claire Dumas, Régine Basseguy, Alain Bergel *

Laboratoire de Génie Chimique CNRS-INPT, 5 rue Paulin Talabot, BP 1301, 31106 Toulouse Cedex 1, France

Received 16 July 2007; received in revised form 15 October 2007; accepted 26 October 2007
Available online 7 November 2007

Abstract

Biofilms of *Geobacter sulfurreducens* were grown on graphite and on dimensionally stable anodes (DSA) in medium that did not contain any soluble electron acceptor. Several working electrodes were individually addressed and placed in the same reactor to compare their electrochemical behaviour in exactly the same biochemical conditions. Under constant polarization at 0.20 V versus Ag/AgCl, the electrodes were able progressively to oxidize acetate (5 mM), and average current densities around 5 A m^{-2} and 8 A m^{-2} were sustained for days on DSA and graphite, respectively. Removing the biofilm from the electrodes led the current to zero, while changing the medium by fresh one did not disturb the current when contact to air was avoided. This confirmed that the biofilm was fully responsible for the electro-catalysis of acetate oxidation and the current was not due to the accumulation of compounds in the bulk. Cyclic voltammetries performed during chronoamperometry indicated that the oxidation started above 0.05 V versus Ag/AgCl. The difference in maximal current values obtained with DSA and graphite was not linked to the biofilm coverage ratios, which were of the same order of magnitude in the range of 62–78%. On the contrary, the difference in maximal current values matched the ratio of the average surface roughness of the materials, 5.6 μm and 3.2 μm for graphite and DSA, respectively.

Keywords: Electroactive biofilm; *Geobacter sulfurreducens*; Dimensionally stable anode (DSA); Surface roughness; Microbial fuel cell (MFC)

1. Introduction

Production of electrical current from electrodes placed in microbial cultures was observed nearly a century ago [1]. Attempts to convert the chemical energy of organic matter directly into electrical energy with microbial fuel cells (MFC) were subsequently explored throughout the 20th century [2,3]. The first cells have generally coupled the microbial production of reduced compounds that were further used as reactant for abiotic electrochemical oxidation on the anode surface. This type of fuel cell, which coupled problems related to both microbial fermentation and abiotic electrochemical reaction, were not successful in their day. The discovery at the beginning of the 21st century of bacteria that can transfer the electrons, issued from their metabolism, directly onto solid anodes, represented a basic breakthrough [4–6] which has considerably enhanced MFC power output [7]. Several reviews have been proposed in the recent flourishing literature on the subject [8–10]. Bacteria isolated from natural consortia have been demonstrated to be able to use an anode as unique electron acceptor without the need for artificial electron mediators. Pure cultures of *Geobacter sulfurreducens* [11], *Geobacter metallireducens*, *Desulfuromonas acetoxidans* [4], *Rhodoferax ferrireducens* [5], *Shewanella putrefaciens* [6], *Clostridium butyricum* [12], *Aeromonas hydrophila* [13], *Desulfobulbus propionicus* [9] can thus catalyze the electrochemical oxidation of organic compounds such as acetate, glucose, lactate or alcohols.

Numerous studies have aimed at improving electrode materials, cell design and operating conditions to increase MFC efficiency, mainly with natural microbial consortia [14]. Several types of graphite and carbon anodes have been tested to enhance anode performance: carbon granules [15], carbon cloth and foam [5,16], vitreous carbon [17,18], carbon modified with manganese ions or neutral red [19]. Mn^{4+} modified woven graphite used in a one-compartment MFC with sewage sludge led to 1.75 A m^{-2} current density and 787.5 mW/m^2 power density [19]. The influence of the proton exchange

* Corresponding author.
E-mail address: Alain.Bergel@ensiacet.fr (A. Bergel).

doi:10.1016/j.electacta.2007.10.066

membrane (PEM) has been highlighted in an MFC fed with wastewater. Power output was 28 mW/m^2 with the membrane, while it reached 146 mW/m^2 when it was removed. With the addition of glucose, removing the PEM increased power density from 262 mW/m^2 to 494 mW/m^2 [7]. The influence of various operating parameters was assessed in a membrane-less MFC: increasing the solution's ionic strength from 100 mM to 400 mM by addition of NaCl resulted in power output increasing from 720 mW/m^2 to 1330 mW/m^2. Power generation went from 720 mW/m^2 to 1210 mW/m^2 by decreasing the distance between anode and cathode from 4 cm to 2 cm [20].

Cyclic voltammetry (CV) has been carried out to advance understanding of microbial electrocatalysis mechanisms, but most of these studies investigated suspensions of microbial cells [12,13,21–24] or freshly adherent micro-organisms [25]. CV on mature biofilms has been more rarely reported [26].

Several studies have implemented constant potential chronoamperometry with pure cultures to focus on the anode process [6,11,21]. In such conditions, i.e. the working electrode polarized at 0.20 V versus Ag/AgCl, current density values of 0.07 A m^{-2}, 0.25 A m^{-2} and 0.15 A m^{-2} have been sustained with *R. ferrireducens* [5], *G. metallireducens* [4] and *D. acetoxidans* [4] biofilms, respectively. *G. sulfurreducens* biofilms gave the highest current densities in the range of 0.16–1.14 A m^{-2} on graphite anodes [11].

The purpose of the present work was to assess the capacity of dimensionally stable anode (DSA) to grow effective electrochemically active biofilms and to compare them with graphite anodes, which are commonly used in literature. DSA electrodes are made of a titanium base covered by metal oxides (iridium and tantalum oxides in our case). They have revealed remarkable electrocatalytic properties in many industrial processes such as chlorine, oxygen or hydrogen evolution as well as organic oxidations [27]. They are very stable electrodes even in aggressive media, and are industrially produced in form of plates, nets, meshes, expanded metals, etc. They can be packed more compactly than massive and bulky graphite electrodes, which is a preponderant advantage when increasing the surface area is the key parameter. If they revealed effective in growing electrochemically active biofilms, they would be excellent candidates for scaling up industrial MFC pilots. It may be noted that DSA has already been used successfully in a microbial-catalyzed denitrifying process, but the nitrate-reducing micro-organisms were grown on graphite cathode, and DSA only played the role of an abiotic auxiliary electrode [28]. DSA has also been used successfully to grow electrochemically active biofilms in garden compost [29].

With the view to work in rather standard conditions, similar experiments as presented in Ref. [11] were repeated here: pure cultures of *G. sulfurreducens* were grown with acetate as electron donor in a medium where the anodes, polarized at 0.20 V versus Ag/AgCl, were the sole electron acceptors. The reactors were equipped with several individually addressed working electrodes. This technique, which was implemented here for the first time on microbial electrochemistry, avoided the discrepancies that may be induced by the biochemical conditions. It should be now more systematically used when comparing different electrode materials.

2. Experimental

2.1. Media and growth conditions

G. sulfurreducens strain PCA (ATCC 51573) was purchased from DSMZ (Deutsche Sammlung von Mikroorganismen und Zellkulturen). The growth medium contained (per litre): 0.1 g KCl, 1.5 g NH_4Cl, 2.5 g $NaHCO_3$, 0.6 g NaH_2PO_4, 0.82 g acetate, 10 mL vitamin mix (ATCC MD-VS), and 10 mL trace mineral mix (ATCC MD-TMS). The medium was autoclaved and completed with a filtered (0.2 μm) solution of sodium fumarate for a final concentration of 8 g/L.

Incubations were done at 30 °C during 5 days in the incubation medium. The number of planktonic cells was evaluated through the absorbance at 620 nm. Absorbance was transformed into cell forming units per millilitre (CFU mL^{-1}) using the calibration formula:

$$[\text{CFU mL}^{-1}] = \text{OD}_{620\,\text{nm}} \times 472,067 \quad (1)$$

established with measurements in Petri dishes under a N_2/CO_2 atmosphere.

The reactor medium, used in the electrochemical reactor, was the same as the incubation medium, except that it lacked sodium fumarate and contained sodium acetate at a final concentration of 0.41 g/L (5 mM). After its transfer into the reactor, this reactor medium was flushed with N_2–CO_2 (80–20%) to remove oxygen for at least an hour, the flow was then reduced during the experiments. Cells (5%, v/v) were then injected into the electrochemical reactor when the optical density at 620 nm in the incubation medium was around 0.3 (i.e. around 142,000 CFU mL^{-1}).

2.2. Electrodes and reactor

The electrochemical reactor contained approximately 2 L of reactor medium with a 0.5 L headspace (total volume = 2.5 L). The top of the reactor comprised seven sampling ports, and the body two inlet and outlet ports. The junction between the top and the body of reactor was sealed with a clamping ring. Sampling ports were sealed with butyl stoppers. Each electrode was drilled, tapped and a titanium wire was screwed into them to ensure the electrical connection. The titanium wires were shielded with thermoretractable sheaths and were introduced from the top through a holed seal in the sampling port. The electrodes were 5 cm × 2.5 cm × 0.5 cm sheets of graphite (Goodfellow), and 5 cm × 2.5 cm × 0.1 cm, 4.5 cm × 2.5 cm × 0.1 cm or 2.5 cm × 1 cm × 0.1 cm sheets of dimensionally stable anodes (DSA, ECS International Electrochemical Services).

Before each experiment, graphite electrodes were washed for an hour in 1N HCl, and another hour in 1N NaOH to remove possible biomass contamination. DSA were electrolysed at 200 A m^{-2} for 5 h in 0.1 M H_2SO_4. Counter electrode

Table 1
Operating parameters and main results from the five reactors

Reactor number	Name	Surface area (cm^2)	10% of maximum current density (day)	Day of maximum current density	Maximum current density ($A\,m^{-2}$)	Stability days (75% of maximum current density)
1	DSA.1.1	12.5	3.4	5.7	4.8	4 → 8
	DSA.1.2	11.5	3.6	5.7	5	5 → 8
2	GR.2.1	12.5	0.5	3	7.8	1 → 5
	GR.2.2	12.5	0.5	2	8 (saturation)	1 → 5
3	GR.3.1	12.5	1.4	5	8	2 → 7
	DSA.3.1	12.5	2	5	5.3	3 → 7
4	DSA.4	2.5	5.4	14.7	8.3	10.7→
5	DSA.5	2.5	5	15.6	8.4	10.8→

was a platinum grid made up with 0.5 mm diameter wires (90% Pt–10% Ir, Platecxis). The platinum grid was cleaned by means of red-hot heating flame. The Ag/AgCl reference electrode was made with a 1.5 mm diameter silver wire dipped into a HNO_3 solution and then immediately transferred into saturated KCl.

2.3. Electrochemical measurements

Electrochemical experiments were carried out using one to three working electrodes (graphite or DSA) dipped in the same reactor and connected to the same auxiliary (platinum grid) and reference electrodes through a multi-potentiostat (model VMP1 or VMP2, software EC-Lab v.8.3, Bio-Logic SA). A silver/silver chloride (Ag/AgCl) electrode was used as reference, and all potential were expressed with respect to this reference throughout the paper. The potential of the reference electrode in the reactor medium was around $E_{(Ag/AgCl)} = 0.31$ V/SHE. Each working electrode was monitored independently by means of an N-STAT device (Bio-Logic SA). Control samples of electrode materials were sometimes placed in the reactor but not connected to the electrochemical set-up. The working electrodes were maintained at 0.20 V and current was recorded every 300 s. Acquisition was suspended periodically to perform cyclic voltammetries (CVs) at $2\,mV\,s^{-1}$ or $10\,mV\,s^{-1}$. At the end of experiments, electrode surfaces were observed by epifluorescence microscopy. In some cases, the biofilm was removed from the electrode surface by scratching it with paper wet with ethanol, the electrode was then rinsed with distilled water and replaced in the reactor medium for performing CV.

2.4. Microscopy methods

2.4.1. Epifluorescence microscopy

At the end of experiment, electrodes were removed from the reactor, stained with a solution of 0.03% orange acridine (A6014, Sigma) for 10 min, then rinsed with distilled water and air dried. Unless otherwise stated, pictures were taken using a Carl Zeiss Axiotech 100 microscope equipped for epifluorescence with HBO 50/ac mercury light source and Zeiss 09 filter (excitor AP 450-490, reflector FT 510, barrier filter LP 520). Image acquisition and processing was achieved with a monochrome digital camera (Evolution VF) and the software Image-Pro Plus v.5.

2.4.2. Scanning electron microscopy

Scanning electron microscopy was accomplished on clean electrodes after pre-treatment (protocol described in Section 2.2). Image acquisition was effected with a SEM LEO 435 VP (diaphragms used were 30 μm, 50 μm and 700 μm). Data were analysed using LEO UIF software.

2.4.3. Surface roughness analysis

The surface morphology and roughness of the clean electrodes (protocol described in Section 2.2) were characterized using a white light interferometer Zygo New View 100 OMP-0348K monitored with a MetroPro software. The measurements were carried out with a sampling distance of 100 μm from the coupon surface for both electrode materials. Surface topographies with features up to 100 μm high can be determined with a vertical resolution down to 0.1 nm. The method was used to characterize the average roughness (R_a) of the surfaces.

3. Results and discussion

The electrodes (pre-treated as described in Section 2.2) were placed in reactors containing 2 L (reactors 1–3) or 0.5 L (reactors 4 and 5) sterile reactor medium and were individually polarized at 0.20 V versus Ag/AgCl. The reactors were inoculated (5%, v/v) with *G. sulfurreducens* previously grown in incubation medium for 5 days at 30 °C. Cyclic voltamogramms (CV) were recorded just before inoculation and then periodically during the experiment. Five experiments were carried out following the same procedure. A few coupons that were not polarized were also set in some reactors. All electrodes showed the same general shape of current evolution, as represented in Fig. 1: an initial lag period followed by sigmoid increase and final stabilisation. The parameters describing the curves were gathered in Table 1: the day when 10% of maximum current density was reached, the day when current density achieved its maximum value, maximum current density and current stability, i.e. the period when current density remained higher than 75% of its maximum value.

3.1. DSA and graphite anodes under chronoamperometry

The two dimensionally stable anodes (DSA) implemented in reactor 1 exhibited exactly the same evolutions in current

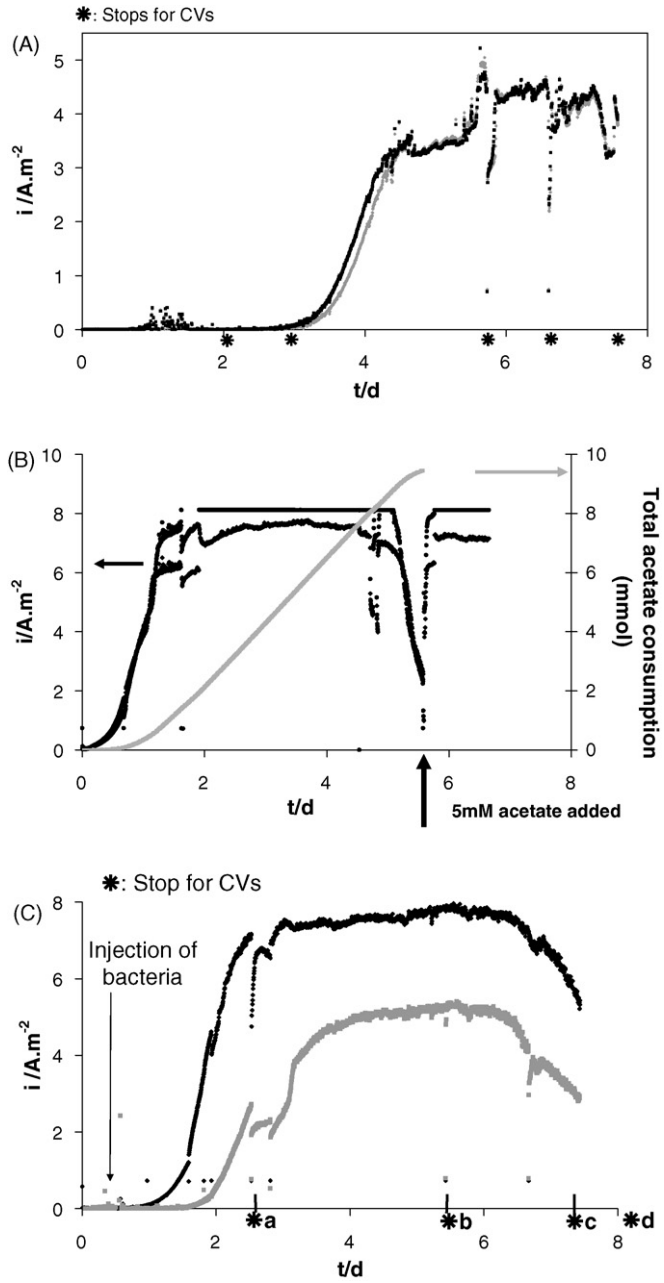

Fig. 1. Evolution of the current density with time on DSA and graphite electrodes exposed to *Geobacter sulfurreducens* culture and polarized at +0.20 V vs. Ag/AgCl. Injection of 5% (v/v) of bacteria; medium containing 5 mM acetate as electron donor and no electron acceptor; stars (✱) indicate the interruptions for CV recording. (A) Reactor 1 with two DSA electrodes (■: DSA1.1; ♦: DSA1.2), bacteria inoculated at day 0. (B) Reactor 2 with two graphite electrodes (GR2.1 and GR2.2), bacteria inoculated at day 0. The acetate consumption (mmol) was derived from current integration. (C) Reactor 3 with a DSA and a graphite electrode (■: GR3.1; ◆: DSA3.1), bacteria inoculated at day 0.12 (i.e. 3 h).

density versus time (Fig. 1A) although they were individually addressed. The current started to increase a few days after inoculation, reaching an average plateau around 4.4 A m^{-2}, which remained stable for more than 2 days, with maximum peaks up to 4.8 A m^{-2}.

Two graphite anodes were tested in the same way in reactor 2. Current density began to increase after only 1 day of culture, reaching a maximum value in the range 7.5–8 A m^{-2} after 2 or 3 days for both electrodes (Fig. 1B). This maximum value was limited for electrode GR2.2 because of the saturation threshold of the electronic set-up at 10 mA. Current density was stable for 4 days and dropped dramatically on day 5. It has been demonstrated in the same conditions that *G. sulfurreducens* oxidizes acetate to CO_2 with eight electrons exchanged:

$$CH_3COO^- + 4H_2O \rightarrow 8e^- + 2HCO_3^- + 9H^+ \quad (2)$$

transferring directly these electrons to the anode [11].

Assuming the same reaction pathway, the number of mole of acetate consumed by electrochemical reaction was derived from the integration of the current supplied by the two electrodes, as reported in Fig. 1B. Current integration indicated that around 9 mmol acetate should be consumed at day 5, which suggests that the current decrease starting at this date was due to acetate depletion. According to current integration, the 10 mmol acetate that were contained initially in the reactor (5 mM in 2 L medium) should be completely consumed at day 5.6, exactly when current fell to zero. Addition of 5 mM acetate to the medium, made the current density fast increase close to maximum value, confirming that the current decrease was due to the complete consumption of acetate. These results are consistent with the high coulombic efficiency of *G. sulfurreducens* in catalysing the electrochemical oxidation of acetate, as already reported (98.6%) [11]. It must be noted that the current decrease was sudden and sharp; it did not reveal the gradual decrease proportional to the concentration of reactant that would be expected for a common batch electrolysis. Such behaviour has already been observed with microbial electrocatalysis [11]. It should be drawn that the rate of microbial electrocatalysis is not controlled by a common electrochemical kinetics, but rather by a kinetics related to the metabolic processes of the adherent cells, which should not be directly proportional to the concentration of the substrate (here acetate).

The differences in current densities obtained with graphite and DSA electrodes were confirmed by implementing in the same reactor two electrodes of different materials (reactor 3, Fig. 1C). The graphite anode led to higher current, around 8 A m^{-2}, while DSA sustained around 5.3 A m^{-2}. As observed by comparing reactors 1 and 2, the growth phase confirmed to be faster on graphite.

3.2. Medium changing experiments

Experiments 4 and 5 were carried out in a 0.5 L reactor with only one 2.5 cm^2 DSA electrode in each reactor, following the same general procedure. In the experiment 4 (Fig. 2A), the current density increased to 4.3 A m^{-2} and was around 2.3 A m^{-2} at the end of day 9. The electrode was then removed from the reactor and placed in a new one, previously filled with fresh deoxygenated medium (N_2/CO_2). No new inoculation was done. As previously reported [11], current fell to a basal level but restored rapidly. In this second reactor, the current increased to 7.4 A m^{-2} after 1 day, then stabilising at values higher than 8 A m^{-2}. Stirring for 1 day with a magnetic barrel did not have

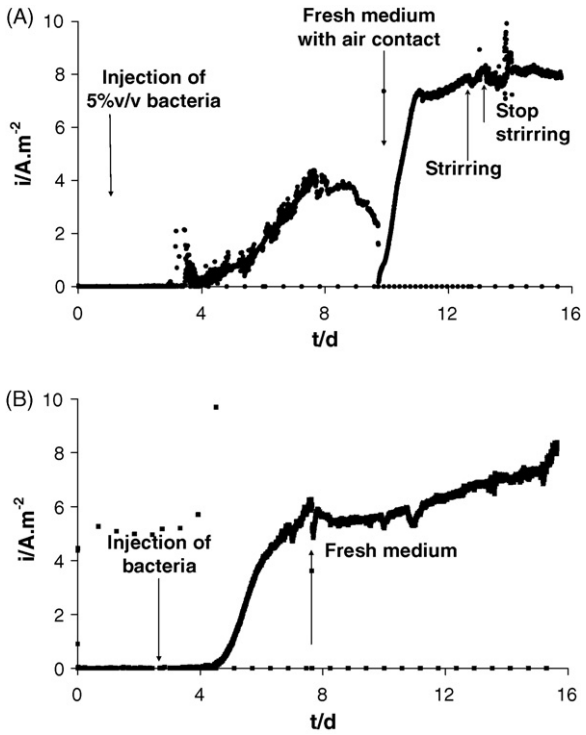

Fig. 2. Evolution of the current density with time on DSA electrodes polarized at +0.20 V vs. Ag/AgCl exposed to *G. sulfurreducens* culture, and effect of medium renewal by a fresh one (with 5 mM acetate as electron donor and no electron acceptor). (A) Electrode was taken out of the reactor 4 and placed in a fresh medium. Air–contact was not avoided. (B) Electrode was kept in the reactor 5 under N_2/CO_2 atmosphere during the medium replacement.

any effect on the current value, indicating that mass transfer of acetate in the solution was not a rate limiting step.

In experiment 5, when the current was stabilised around 6 A m^{-2} (Fig. 2B), the reactor was purged keeping it below the N_2/CO_2 atmosphere. It was immediately refilled with fresh medium that had previously been deoxygenated so as to avoid contact with air. In this case, the current was not disturbed by the change in medium. The sharp current decrease that was observed in the previous experiment should consequently be due to transient introduction of air into the reactor. This last experiment also pushed away the assumption that hydrogen resulting from water electrolysis on the auxiliary electrode might oxidize on the biofilm-covered anode, and so increase artificially the current measured [30]. Moreover, all experiments were performed here under continuous N_2/CO_2 bubbling in order to avoid this possible artefact due to hydrogen cycling.

In reactors 4 and 5, the current densities obtained in the fresh media were always higher than the ones obtained in previous experiments. It may be explained by the occurrence of antagonist phenomena: (i) the increase of biofilm effectiveness with time, due to the increase of the number of active cells or to higher electron transfer rates, (ii) the depletion of acetate and (iii) accumulation of products and metabolites in the bulk that may inhibit the active cells. Before medium renewal, the slow decrease in acetate concentration and possible accumulation of inhibiting compounds may be more or less balanced by the slow increase in biofilm effectiveness. This resulted in a current density plateau. The medium renewal restored the acetate concentration at the initial value of 5 mM and may also remove possible inhibiting compounds, the intrinsic effectiveness of the biofilm was no longer masked by the operating conditions and it was consequently able to supply maximal current values.

3.3. Cyclic voltammetry (CV) on DSA and graphite anodes

CV performed at 10 mV s^{-1} on the graphite electrode (GR2.2, Fig. 3A) at day 0 just before bacteria injection in the reactor 2 showed a clear redox peaks around −0.44 V (−0.13 V/SHE). Their height proportional to scan rate (data not shown) indicated a redox system due to adsorbed compounds, certainly coming from the culture medium. CV performed at 10 mV s^{-1} on day 0.8 (i.e. 19 h) during current increase, when the electrode sustained 2.5 A m^{-2}, revealed two new redox couples at −0.075 V and +0.150 V (0.235 V/SHE and 0.460 V/SHE, respectively). It has been proved that several outer membrane cytochromes play a key role in the direct electron transfer of *G. sulfurreducens* to solid electrodes [31]. The cytochrome *c* OmcS has been demonstrated to be involved in the electron transfer to solid electrodes [31] but, to our knowledge, its redox potential has not been determined yet. A redox potential of −0.167 V/SHE has been reported for another *G. sulfurreducens* periplasmic and extracellular cytochrome involved in the Fe(III) reduction [32]. Even if this redox potential has been determined by titration in quite different conditions, the values found here, with more than 400 mV difference, did likely not correspond to this cytochrome. The genome of *G. sulfurreducens* encodes 111 *c*-type cytochromes, which represents a significantly higher number than for all other micro-organisms whose sequence is available [33]. The peak observed here could thus be related to another *c*-type cytochrome or to redox proteins also involved in the electron transfer chain, as already demonstrated [34].

As the current increased during chronoamperometry, a high oxidation current appeared on the CV, which increased and logically masked the peak at −0.075 V. Fig. 3B reports CV performed at 2 mV s^{-1} on the graphite electrode at day 2 when the electrode (GR2.1) sustained 6.9 A m^{-2}. At the end of the experiment, the biofilm was removed from the electrode and put back to the reactor, any oxidation process disappeared. As it has already been shown in a different way [11] the biofilm-driven catalysis was responsible for the whole oxidation reaction and neither planktonic cells nor metabolites were involved in this oxidation process. On the contrary, the reduction reaction, which occurred on both the biofilm-covered and the cleaned electrodes, was certainly due to the reduction of a metabolite produced during electrolysis. In literature, similar oxidation signals have already been observed with biofilms formed in different MFC. A biofilm-covered electrode, formed in a MFC containing potato-processing sludge, revealed redox peaks centred at 0.18 V versus Ag/AgCl when placed in cell-free media, showing that the redox couple was embedded within the biofilm [25]. Similarly, a MFC inoculated with domestic wastewater and fed with acetate revealed peaks around −0.30 V versus Ag/AgCl, which disappeared on CVs carried out in the same solution after biofilm removal from the anode surface [26].

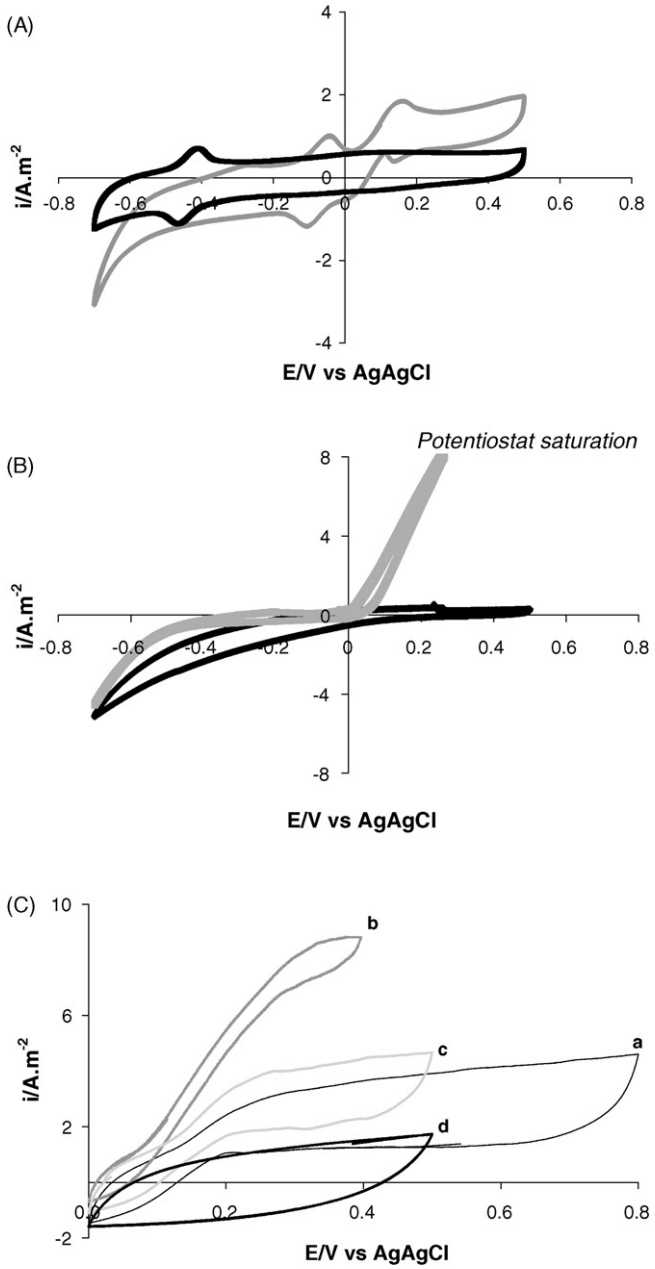

Fig. 3. Cyclic voltammetries performed during the chronoamperometry experiments. (A) Reactor 2: graphite GR2.2 at 10 mV s^{-1} before bacteria injection (■) (day 0) and after bacteria injection (◆) (day 0.8, i.e. 19 h). Current density sustained on day 0.8 ≈ 2.5 A m^{-2}. (B) Reactor 2: graphite GR2.1 at 2 mV s^{-1} with biofilm (■) on day 2 and after cleaning (♦) on day 8. Current density sustained on day 2 ≈ 6.9 A m^{-2}. CV with the biofilm covered electrode was stopped at a lower upper limit because of the saturation threshold of the potentiostat. (C) Reactor 3: DSA3.1 at 2 mV s^{-1} with a biofilm aged of 2 days (a), 5 days (b), 7 days (c) and after biofilm was removed (d). Biofilm sustained (a) 2.5 A m^{-2}; (b) 5.2 A m^{-2}; (c) 2.8 A m^{-2}.

Fig. 3C depicts the CV performed in reactor 3 at 2 mV s^{-1} on the DSA electrode at days 2, 5, 7, and at the end of the experiment with the cleaned electrode dipped again in the reactor medium. The cleaned electrode revealed the common characteristic behaviour of DSA with the charge and discharge of the oxide surface species, without any contribution from dissolved species [35]. In the presence of the biofilm, the scans revealed a superimposed faradic behaviour, which logically followed evolution in current values that were sustained during chronoamperometry: high current on CV performed at days 2 and 5 and a low current on CV at day 7. As in the case of graphite, the presence of the biofilm was responsible for the whole faradic process. CV performed at 10 mV s^{-1} with DSA did not reveal any redox peak, as was the case with graphite, certainly because of the high charge–discharge basic current. Graphite seems consequently more suitable to carry out analytical studies with the objective to decipher electron transfer pathways. The present work indicated that performing CV during biofilm formation under chronoamperometry may be a promising way in this objective, mainly during the first phase of biofilm growth, as the catalytic effect when increasing tends to mask the small peaks due to adsorbed species.

The different experiments revealed the same behaviour of the biofilms in CVs. Oxidation on DSA started at around 0.05 V and showed a plateau from around 0.35 V. Oxidation started at identical potential values on graphite, with a peak observed at −0.075 V at the beginning of biofilm formation. CV performed in suspension of *G. sulfurreducens* cells have reported in literature, which exhibited an oxidation peak at fairly lower potential values, around −0.20 V versus Ag/AgCl [36]. Nevertheless in this study, cells were suspended in solution and they were grown with Fe(III) as electron acceptor instead of fumarate as done here. It may be suggested that the electrochemical features of *G. sulfurreducens* may be pretty versatile, depending on the operating conditions (composition of the culture medium, nature of the electron acceptor, CV recorded with biofilm-coated electrode or with cell suspension, etc.).

3.4. Assessment of coverage ratios

DSA control coupons that were not connected were placed in reactors 2 and 3. A typical picture obtained by epifluorescence microscopy is reported in Fig. 4. The numerical post-treatment was performed by choosing a threshold in light intensity that divided images into two classes: highly fluorescent areas that reveal bacterial colonization (in white on the post-treated pictures), and low light zones (black in the post-treated pictures) that correspond to non-colonized areas. The biofilm coverage ratio was defined as the ratio of the white area with respect to the total area analysed. The error on the biofilm coverage ratio was assessed by varying the threshold of light intensity, while keeping a representative post-treated image with a visual aspect close to the initial picture. It was only ±2%. Pictures were taken on five different spots on each electrode, and an average coverage ratio was extracted with a standard deviation of 2.5%.

The DSA control coupons (not connected) showed scattered bacteria (Fig. 4) and small colonies with average coverage ratios of 12% (reactor 2, not shown) and 8% (reactor 3, Fig. 4). A control coupon of graphite in reactor 3 showed the same scattered bacteria and small colonies with a coverage ratio of 7.4%. The raw pictures revealed light grey areas due to parasite fluorescence, which was probably induced by mushroom-like exopolymer structures that grew above the surface, as particularly visible on Fig. 4. The numerical treatment revealed very

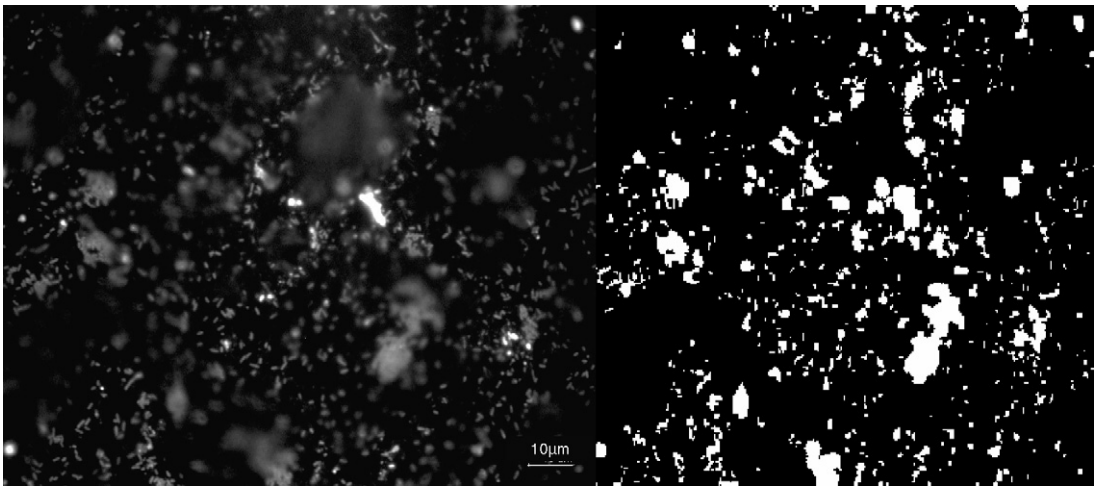

Fig. 4. Microscopic pictures of *G. sulfurreducens* biofilm on control DSA coupon (DSA 3.2) not connected; magnification 500× and numerical post-treatment. White: biofilm-covered surface area (8%), black: free electrode surface area.

efficient in "cleaning" the image from these super-structures, leading to an assessment of the actual coverage ratio.

In the absence of electron acceptor in the reactor medium, the presence of colonies on the surface of not connected coupons was unexpected. It may be assumed that the low colonization observed on the control coupons may be due to the detachment of cells from the anodes contained in the reactor and/or to a basal growth that was maintained by the residual amount of fumarate contained in the inoculum volume. Recording absorbance of the medium as a function of time in reactor 3 indicated a slow continuous growth of planktonic biomass (Fig. 5). Nevertheless, the amount of planktonic cells, around 35,000 CFU mL^{-1} at the maximum, remained low, confirming that it was only a residual growth. This residual growth diverted a part of the metabolic process from the electron transfer to the electrode.

The connected anodes showed dense biofilms settled on the whole surface area, as shown in Fig. 6 (DSA1.1 and DSA1.2 from reactor 1, which produced 4.8 A m^{-2} and 5 A m^{-2}, respectively). The bacteria formed dense aggregates around 10–20 µm diameter and developed colonization on the whole surface with polymer matrix rising above the focal plan. Defining a strict frontier between colonized and non-colonized areas was less easy, because there were fluorescent cells at several planes above the surface level where the image was focalised, and parasitic fluorescence also resulted from basal adsorption of the staining dye on the biofilm matrix. The assessed error in choosing the light threshold was here of ±7% instead of ±2% for non-connected coupons and a standard deviation of 5%. The anode DSA1.1 showed a coverage ratio of 87% when treated at magnification 100× (Fig. 6A). Magnification 500× lead to a more detailed view and allowed the numerical treatment to make a better distinction between residual light and the fluorescent due to the cell on the electrode surface. The coverage ratio was thus 62% for DSA1.1 (Fig. 6B) and 78% for DSA1.2 (picture not shown). The biofilm formed on a graphite electrode from reactor 2 that sustained 8 A m^{-2} at the end of the experiment had a coverage ratio of 75% and was similar in morphology to the biofilms formed on DSA electrodes. The preponderant part of the biofilm, stained with orange acridine, was green fluorescent (DNA) showing that most part of the bacteria was no longer active, which is logical as the biofilm spent many hours in aerobic condition when analysis were performed.

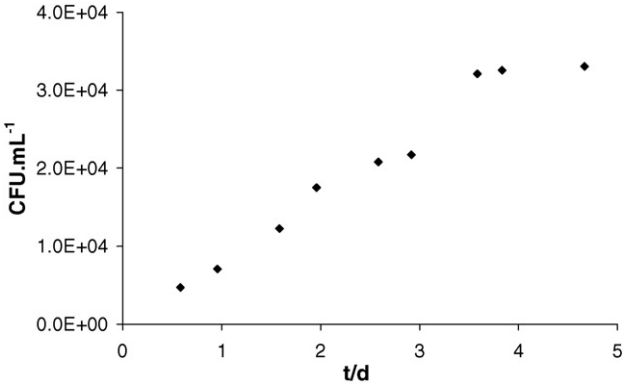

Fig. 5. Evolution of CFU mL^{-1} with time in reactor 3. Absorbance measurements were performed at 620 nm.

As a conclusion, the similar biofilm coverage ratios that were obtained on both DSA and graphite anodes cannot explain the significant differences in the current densities that provided both electrodes. In the bibliography, establishing correlations between the current density values and biofilm morphologies or coverage ratios is still in its infancy. The protein quantity contained in the biofilm is an interesting parameter to be correlated with current density [11,30] but it requires scratching the biofilm and cannot give an indication on biofilm coverage ratio. SEM has the great advantage to give detailed pictures, but biofilms have to undergo several dehydrating and preparation steps, which may induce significant modifications in the biofilm structure [7,11]. Here a simpler technique was proposed, which only required a classic microscope, and appeared to give correct assessment of biofilm coverage ratios. Confocal laser scanning microscopy (CLSM) could also be used to perform this method and it seems to be the most elegant technique with the view to

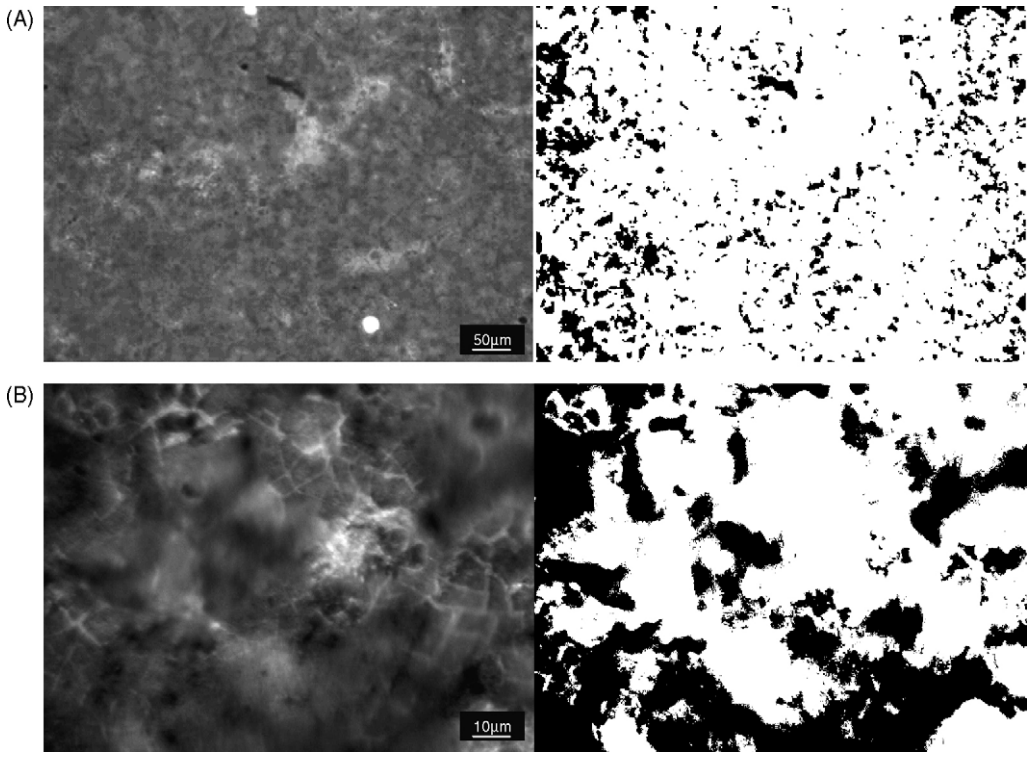

Fig. 6. Epifluorescence microscopy pictures of *G. sulfurreducens* biofilm on DSA electrodes polarized at +0.20 V vs. Ag/AgCl in reactor 1 (DSA1.1) biofilm sustained 4.8 A m^{-2}. (A) Magnification 100×, biofilm-covered surface area 87%. (B) Magnification 500×, biofilm-covered surface area 62%.

investigate *in situ* biofilm morphology and coverage ratios [30] or even to evaluate biofilm thickness [37].

3.5. Morphology of electrode surfaces

Fig. 7 shows SEM pictures of graphite and DSA electrodes (magnification 2500×). Graphite and DSA appeared as rough materials with heterogeneities which seem slightly smaller on graphite. The fine roughness profiles were determined thanks to a light interferometer. The amplitude between the highest and the lowest points of the electrode surface was around 74 µm for graphite and 35 µm for DSA. Average roughness (R_a) was equal to 5.6 µm for graphite and 3.2 µm for DSA. The graphite used here was 1.75 times rougher than the DSA surface, while the current density values (expressed with respect to the geometric surface areas) at 0.20 V were 1.6 times higher for graphite than DSA (around 8 A m^{-2} against 5 A m^{-2}).

It is known that roughness has a crucial effect on bacterial adhesion. Flint et al. [38] reported that adhesion is favoured by entrapment when surface roughness is close to the diameter of bacterial cells. Fouling could consequently be prevented by smoothing the surface roughness from 0.9 µm to lower values [39]. Scheuerman et al. concluded that the presence of irregularities increased the quantity of *Pseudomonas aeruginosa* and adherent *Pseudomonas fluorescens* on silicone samples, but that a roughness higher than 10 µm had no additional effect [40]. The roughness of the materials presented here were in the order of magnitude of the bacterial dimensions known to be 2–3 µm

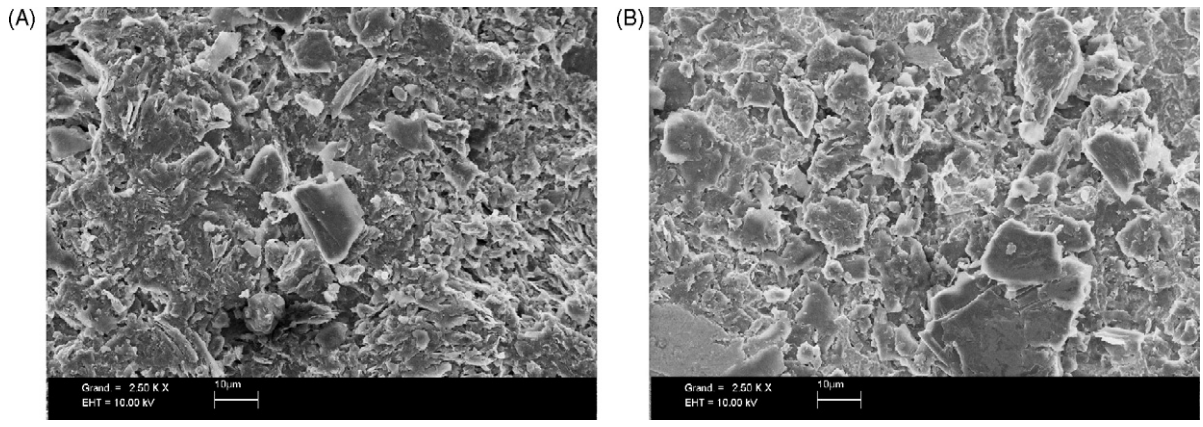

Fig. 7. Scanning electron microscopy (SEM), magnification 2500× on clean electrodes of (A) graphite and (B) DSA.

by 0.5 μm [41]. So, when the material roughness is higher, the number of adhered cells per biofilm covered projected surface area might be increased. Therefore it is coherent that the ratio in current densities between graphite and DSA was controlled by the ratio of material roughness. It may be concluded that the higher efficiency of graphite was mainly explained by the higher surface roughness of the surface than by better kinetic properties of the material.

4. Conclusions

Biofilms of *G. sulfurreducens* developed on graphite and DSA electrodes revealed able to sustain high current densities up to $8\,A\,m^{-2}$ and $5\,A\,m^{-2}$, respectively, which was higher than reported before. Actually, the experiments reported elsewhere, which were not aimed at reaching maximal currents, have certainly been stopped before reaching the maximal values [11]. A numerical treatment of the pictures obtained by epifluorescence microscopy was proposed to estimate *in situ* biofilm coverage ratios. This was the first time that a simple method was proposed to assess the ratio of the surface area covered by the biofilm. Indirect measurements have been proposed (e.g. measuring amount of protein) which requires scratching the biofilm and did not give indication on biofilm coverage. From the practical point of view of current production, the surface coverage ratio is a key parameter, which can be used to assess easily the maximum current density, by simple extrapolation to 100% coverage. This method showed here that the coverage ratios obtained with mature biofilms were very similar for graphite and DSA electrodes that were implemented in identical conditions. It was consequently concluded that the differences in the maximal current density values between graphite and DSA were mainly controlled by the surface roughness.

Because of their technological advantages and the capacity they demonstrated here to grow electrochemically active biofilms, DSA electrodes should constitute a suitable material for scaling up microbial fuel cells. Current densities up to $8\,A\,m^{-2}$ were reached in optimal conditions, i.e. renewing the reactor medium. Optimizing the DSA for MFCs should now progress in increasing their roughness. According to the proportional relationship observed here between roughness values and maximal currents, it may be reasonably hoped that increasing the roughness to 10 μm (limit from which bacterial adhesion was no more affected [40]) should multiply the current by a factor of 3. The similarity between graphite and DSA in terms of maximal current values suggests that the maximal current may be rather independent from their surface composition. Nevertheless, it may be interesting to compare DSA made up with different oxides with the view to shorten the initial growth phase, a feature for which DSA seemed slightly less effective than graphite.

Acknowledgements

This work was financially supported by the Sixth Framework Program of the European Union as part of the project "Electrochemically Active Biofilms" NEST (508866). The authors are very grateful for V. Baylac's help (CIRIMAT -Toulouse) for roughness measurements.

References

[1] M.C. Potter, Proc. R. Soc. (Lond.) B 84 (1911) 260.
[2] H.D. Roller, H.P. Bennetto, G.M. Delaney, J.R. Mason, J.L. Stirling, C.F. Thurston, J. Chem. Tech. Biotechnol. 34B (1984) 3.
[3] S. Suzuki, I. Karube, H. Matsuoka, S. Ueyama, Ann. N. Y. Acad. Sci. 413 (1983) 133.
[4] D.R. Bond, D.E. Holmes, L.M. Tender, D.R. Lovley, Science 295 (2002) 483.
[5] S.K. Chaudhuri, D.R. Lovley, Nat. Biotechnol. 21 (2003) 1229.
[6] B.H. Kim, H.J. Kim, M.S. Hyun, D.H. Park, J. Microbiol. Biotechnol. 9 (1999) 127.
[7] H. Liu, B.E. Logan, Environ. Sci. Technol. 38 (2004) 4040.
[8] D.R. Lovley, Microbe 1 (2006) 323.
[9] D.R. Lovley, Curr. Opin. Biotechnol. 17 (2006) 1.
[10] B.E. Logan, B. Hamelers, R. Rozendal, U. Schroder, J. Keller, S. Freguia, P. Aelterman, W. Verstraete, K. Rabaey, Environ. Sci. Technol. 40 (2006) 5181.
[11] D.R. Bond, D.R. Lovley, Appl. Environ. Microbiol. 69 (2003) 1548.
[12] H.S. Park, B.H. Kim, H.S. Kim, H.J. Kim, G.T. Kim, M. Kim, I.S. Chang, Y.K. Park, H.J. Chang, Anaerobe 7 (2001) 297.
[13] C.A. Pham, S.J. Jung, N.T. Phung, J. Lee, I.S. Chang, B.H. Kim, H. Yi, J. Chun, FEMS Microbiol. Lett. 223 (2003) 129.
[14] K. Rabaey, W. Verstraete, Trends Biotechnol. 23 (2005) 291.
[15] P. Aelterman, K. Rabaey, H.T. Pham, N. Boon, W. Verstraete, Environ. Sci. Technol. 40 (2006) 3388.
[16] E. Zhang, W. Xu, G. Diao, C. Shuang, J. Power Sources 161 (2006) 820.
[17] N. Kim, Y. Choi, S. Jung, S. Kim, Biotechnol. Bioeng. 70 (2000) 109.
[18] N. Kim, Y. Choi, S. Jung, K. Sunghyun, Bull. Korean Chem. Soc. 21 (2000) 44.
[19] D.H. Park, J.G. Zeikus, Biotechnol. Bioeng. 81 (2003) 348.
[20] H. Liu, S. Cheng, B.E. Logan, Environ. Sci. Technol. 39 (2005) 5488.
[21] S.A. Lee, Y. Choi, S. Jung, S. Kim, Bioelectrochemistry 57 (2002) 173.
[22] K. Rabaey, W. Ossieur, M. Verhaege, W. Verstraete, Water Sci. Technol. 52 (2005) 515.
[23] K. Rabaey, N. Boon, M. Hofte, W. Verstraete, Environ. Sci. Technol. 39 (2005) 3401.
[24] Y. Choi, E. Jung, S. Kim, S. Jung, Bioelectrochemistry 59 (2003) 121.
[25] K. Rabaey, N. Boon, S.D. Siciliano, M. Verhaege, W. Verstraete, Appl. Environ. Microbiol. 70 (2004) 5373.
[26] H. Liu, S. Cheng, B.E. Logan, Environ. Sci. Technol. 39 (2005) 658.
[27] S. Trasatti, Electrochim. Acta 45 (2000) 2377.
[28] H.I. Park, D.K. Kim, Y.-J. Choi, D. Pak, Process Biochem. 40 (2005) 3383.
[29] S. Parot, M.-L. Délia, A. Bergel, Bioresour. Technol., in press.
[30] B.E. Logan, J.M. Regan, Trends Microbiol. 14 (2006) 512.
[31] D.E. Holmes, S.K. Chaudhuri, K.P. Nevin, T. Mehta, B.A. Methé, A. Liu, J.E. Ward, T.L. Woodard, J. Webster, D.R. Lovley, Environ. Microbiol. 8 (2006) 1805.
[32] S. Seeliger, R. Cord-Ruwisch, B. Schink, J. Bacteriol. 180 (1998) 3686.
[33] B.A. Methé, K.E. Nelson, J.A. Eisen, I.T. Paulsen, W. Nelson, J.F. Heidelberg, D. Wu, M. Wu, N. Ward, M.J. Beanan, R.J. Dodson, R. Madupu, L.M. Brinkac, S.C. Daugherty, R.T. Deboy, A.S. Durkin, M. Gwinn, J.F. Kolonay, S.A. Sullivan, D.H. Haft, J. Selengut, T.M. Davidsen, N. Zafar, O. White, B. Tran, C. Romero, H.A. Forberger, J. Weidman, H. Khouri, T.V. Feldblyum, T.R. Utterback, S.E. Van Aken, D.R. Lovley, C.M. Fraser, Science 302 (2003) 1967.
[34] E. Afkar, G. Reguera, M. Schiffer, D.R. Lovley, BMC Microbiol. 5 (2005) 41.
[35] Y.E. Roginskaya, O.V. Morozova, G.I. Kaplan, R.R. Shifrina, M. Smirnov, S. Trasatti, Electrochim. Acta 38 (2004) 2435.
[36] J.P. Busalmen, A. Esteve-Nuñez, J.M. Feliu Martinez, Proceedings of the 19th Symposium of Bioelectrochemistry Society, Toulouse, France, poster 27A, 2007.

[37] G. Reguera, K.P. Nevin, J.S. Nicoll, S.F. Covalla, T.L. Woodard, D.R. Lovley, Appl. Environ. Microbiol. 72 (2006) 7345.
[38] S.H. Flint, J.D. Brooks, P.J. Bremer, J. Food Eng. 43 (2000) 235.
[39] L.R. Hilbert, D. Bagge-Ravn, J. Kold, L. Gram, Int. Biodeter. Biodegr. 52 (2003) 175.
[40] T.R. Scheuerman, A.K. Camper, M.A. Hamilton, J. Colloid Interf. Sci. 208 (1998) 23.
[41] F.J. Caccavo, D.J. Lonergan, D.R. Lovley, M. Davis, J.F. Stolz, M.J. McInerney, Appl. Environ. Microbiol. 60 (1994) 3752.